Hindawi
Indoor Air
Volume 2023, Article ID 6359137, 7 pages
https://doi.org/10.1155/2023/6359137

Research Article

Effects of Ionization on the Filtration of Fine and Ultrafine Particles in Indoor Air

Pranav Muthukrishnan [1] **and Faramarz Farahi** [2]

[1]*Georgia Institute of Technology, North Avenue NW, Atlanta, Georgia 30332, USA*
[2]*Department of Physics and Optical Science, University of North Carolina Charlotte, 9201 University City Blvd., Charlotte, NC 28223, USA*

Correspondence should be addressed to Pranav Muthukrishnan; cmpranav@gmail.com

Received 4 February 2023; Revised 25 May 2023; Accepted 15 June 2023; Published 29 July 2023

Academic Editor: Geun Young Yun

As we spend approximately 80% of our time indoors, improving indoor air quality is necessary to lessen the spread and impacts of respiratory diseases and other health issues caused by particle pollution. Currently, in many countries, the primary method of cleaning indoor air is by using better, higher-grade filters in a recirculating air system or increasing ventilation with outdoor air. One way to supplement these time-tested approaches is by implementing ionization. We used a bipolar ionizer to test the removal efficiency of filters on different particle sizes with and without ionization. Calibrated cigarettes were used to generate smoke into a 28-cubic-meter chamber with a recirculating air handling system. It was found that ionization had a 275% increase in the removal efficiency of the most penetrating particle sizes (100-500 nm). We conclude that ionization drastically improves the filter removal efficiency of fine and ultrafine particles in indoor environments.

1. Introduction

Indoor air quality has been a topic of public and scientific discussion for many years. In a comprehensive study published in 2012 by Lim et al., it was estimated that 3.2 million deaths per year are attributed to ambient particle pollution [1]. The World Health Organization confirmed this estimate while increasing the number to approximately 4 million [2]. Additionally, Horton et al. have shown that climate change will substantially increase the frequency and duration of periods of air stagnation in much of the world, thus leading to higher concentrations of particle pollution as well as other air pollutants [3]. Therefore, improving indoor air quality is becoming increasingly pertinent due to the high level of health issues and mortality rates associated with airborne particle pollution.

Among such particle pollution, fine particulate matter ($PM_{2.5}$) has been identified to cause respiratory diseases [4]. Currently, the most effective method to reduce particulate matter indoors is by using air filters together with increased ventilation. Air filters can be implemented in different ways, including in-room air purifiers with filters or heating, ventilation, and air conditioning (HVAC) systems. There is a wide variation in filter efficiency among the air filters used in HVAC systems. Typically, highly efficient filters such as MERV 16 and HEPA filters are associated with a higher pressure drop that increases over time due to additional loading [5] compared to a lower-rated filter such as MERV 6.

All conventional mechanical air filters are made of microfibers that show good efficiency for large particle sizes but with depleted removal efficiency for particles below 500 nm. In particular, around 300 nm is known as the most penetration particle size (MPPS) for most filters. However, this value typically ranges between 100 and 500 nm, depending on the airflow speed at the filter as well as the diameter and fractional volume of the fibers in the filter. These particles within the ultrafine and submicron ranges are the most harmful to humans due to the risk associated with particle deposition in the respiratory system. For example, the typical size range of allergens is between 0.1 and 0.3 μm; for viruses, it ranges between 0.05 and 0.5 μm; and for wildfire

smoke, it is 0.4 to 0.7 μm [6, 7]. As shown in Figure 1 from Kowalski and Bahnfleth, these particle diameter ranges have the lowest filter efficiencies for each of the efficiency curves [8].

In order to improve indoor air quality, it is important to focus on increasing the capture efficiency of these specific particle sizes. Podgorski et al. had found a way to do this by developing and using filters that were composed of nanofibrous as well as microfibrous media [9]. The results of their experiments found that significant increases in filtration efficiency for the MPPS range can be achieved with a moderate rise in pressure drop when utilizing these filters. This method focused on improving the single-fiber deposition efficiency of two of the three mechanisms of deposition (Brownian diffusion and direct interception). The three mechanisms of deposition are impaction, interception, and diffusion; however in addition to improving these three, electrostatic force can also be implemented to improve a filter's performance. This method uses electrostatic interaction between filtration media and particles, therefore, in principle, improving filter performance with no direct effect to the pressure drop. This interaction can be achieved by introducing ions into the air to interact with the particles. The concept of preconditioning particles to increase coagulation has also been used by many others using air ionization [10–17]. All have either used a negative ion generator or a bipolar ion generator.

The focus of this paper is to verify the effect of ionization in improving particle removal efficiency, particularly in the MPPS size range. The data reported is from a series of tests using a bipolar ionizer that is composed of carbon fiber brushes, similar to the systems used by Park et al. as well as Farahi. [14, 15, 18]. The data presented compares the particle removal efficiency of a MERV 10 air filter in an air recirculating HVAC system to that of the same filter when a bipolar ionizer is used to supply both positive and negative ions into the space. The focus of this study is on fine and ultrafine particles [19] produced by a calibrated test cigarette developed by and procured from the University of Kentucky (Kentucky Reference Cigarette # 1 R6F [20]).

2. Experimental Methods

The data presented in this paper was obtained through carefully conducted experiments to examine the effect of needlepoint bipolar ionization on filtration efficiency in a recirculating HVAC system. The current understanding is that when bipolar ionized particles are present in the air, the electrostatic force causes particles of opposite electric charges to attract each other and repel like-charge particles. This attraction-repulsion dynamic is expected to agglomerate ultrafine and fine particles, forming larger particles and thus making it easier for the filter to capture them. This helps to improve the particle removal efficiency of air filters because they typically have very low removal efficiencies for ultrafine and fine particles. The details and conduction of the experiments are described below.

All experiments that are discussed have been conducted in a 28-cubic-meter AHAM room at Blue Heaven Technologies. The air filters used in the trials were 60 cm × 60 cm × 4.5 cm,

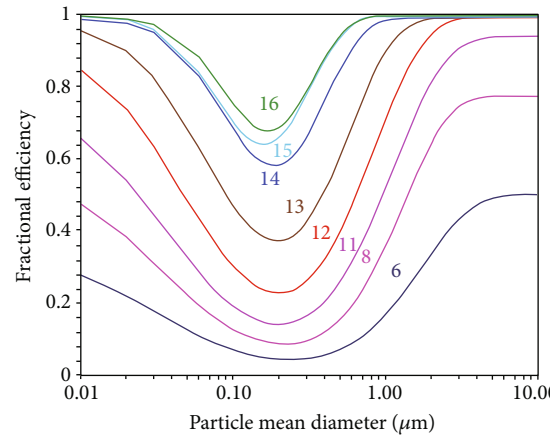

Figure 1: Typical efficiency curve diagram for various rated MERV filters [8].

MERV 10 filters with electret material made by the Aeolus Filter Corporation [21]. The speed of the HVAC recirculating fan was adjusted to achieve 6 air exchanges in the chamber per hour (6 ACH). Following the AHAM standard, a 3-bladed ceiling fan of 36 inches (0.91 m) in length operating at 395 RPM was used to ensure good particle and ion distribution throughout the chamber. A schematic illustrating the experimental setup is shown in Figure 2.

A bipolar ionizer (GPS-FC48™-AC ionization system) that utilizes carbon fiber brushes as ion emitters is mounted in the air supply duct very close to the exit point. The ionizer can be turned on and off remotely as needed. This ionizer has two unipolar electrodes consisting of 48,000 carbon microfibers each, one producing positive ions and the other producing negative ions, with a distance of 2.25 inches (5.625 cm) between them. In order to measure the ion density introduced in the room, an ion counter (Air Ion Counter, AlphaLab, Inc., USA) was mounted on a tripod facing upwards in the middle of the room, 1.5 m from the floor. The ion density was measured in ions/cc of air.

The particle source used was research-grade, calibrated cigarettes from the University of Kentucky that produced a very specific range of particulate sizes from 0.01 to 1.0 μm (PM_1). Researchers have developed methods to introduce a constant level of cigarette smoke into an indoor space [22–25]. As such, the test particles were introduced into the room via the injection port, as shown in Figure 2. This was achieved by attaching a compressed air line to a T-junction. The cigarette was mounted on the second port, and the final port was connected to the tube that feeds into the chamber. Once the cigarette was lit, the compressed air valve is opened, creating a vacuum in the T-junction generated by the forward velocity of the compressed air as it flows through the junction, thus injecting smoke into the chamber. This process ensures an introduction of consistent particle mass and size distribution which is then evenly distributed throughout the chamber using a ceiling fan as previously described.

A TSI DustTrak II Aerosol Monitor and a scanning mobility particle sizer (SMPS) were used to measure the mass and concentration of particles in the chamber. The TSI DustTrak II Aerosol Monitor was placed on the floor

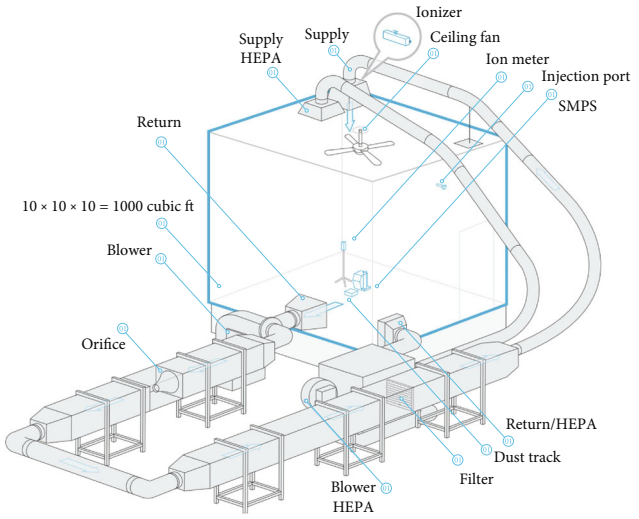

FIGURE 2: Schematic diagram of the experimental setup in which all controls and tests were conducted.

in the middle of the chamber and was used to measure aerosol concentrations corresponding to PM_1, $PM_{2.5}$, PM_{10}, and mass concentrations ranging from 0.001 to 400 mg per cubic meter with a resolution of ±0.1% for particles in the size range of 0.1 to 10 μm. The SMPS (Model 3938 General SMPS, TSI) was used to capture a detailed particle size distribution from 1 nm to 1000 nm with up to 192 channels. The setup for the SMPS included a cyclone sampler linked by conductive tubing to the SMPS, allowing for aerosolized particles in the room to be captured at the cyclone which was located 1 meter above the floor and delivered to the spectrometer. The SMPS measures the concentration of particles with units of particles per cubic centimeter (#/cc) for particle sizes ranging from 1 nm to 1000 nm recorded as a function of time.

In conducting the experiments, a new filter was first tested with the ionizer turned off. A calibrated cigarette was then used to produce airborne particles, as previously described. Data, including particle counts for various bin sizes and particle mass, was collected over the course of 16 hours. This run will be referred to as the "control" run. Following the control test, the chamber walls were wiped, and a second, separate air recirculating system with a HEPA filter was used to clean the air in the room, as recommended by AHAM. Once the room was cleaned, the recirculating system with the MERV 10 filter was reactivated, the ionizer was turned ON, and the smoke particles were introduced once again. The same data was taken over 16 hours. This run will be referred to as the "treatment" run. These steps were repeated three times with a new filter each time.

In general, such experiments would need to be conducted in a bi-directional crossover fashion, as we know that pre-loading of the filter media will affect the performance of the system. However, this is only impactful if the loading for each trial is high. To confirm this, multiple experiments were executed, sometimes in the reverse order, where we started with the treatment runs first, followed by the control runs. We observed no measurable effect on the results because the particle loading was so low. This is due to the fact that loading from one cigarette had no measurable impact on the filter's performance.

The data used in this paper are from three control and treatment trials in which all conditions were the same except for a new air filter used for each set of control and treatment runs. For the purpose of analysis, the control data used was the average of the three control tests.

3. Theory

In order to properly compare the removal efficiencies for different particle sizes, there must first be a way to model efficiency curves based on properties of the filter such as fiber diameter, thickness, particle speed, and fractional volume of the fiber. There are three main mechanisms that determine filtration efficiencies: diffusion, interception, and impaction [26]. Diffusion is the removal process that dominates when the particle diameter is less than about 0.1 μm [26]. In this particle diameter region, Brownian motion occurs causing the particles to randomly traverse large areas respective to their size which allows for them to attach to a filter fiber. Interception occurs predominantly for particle sizes above 0.1 μm. In this process, a particle is following a normal airflow streamline until it is captured by a fiber in the filter through natural forces [26]. Impaction occurs in much larger particle sizes when a particle's inertia is high enough that it cannot adjust to the changes in the airflow streamline, and so it impacts the filter and is captured [26]. Impaction, however, does not make a significant impact on filter removal efficiency for normal filter velocities [26], and thus it will not be included in the modeling of efficiency curves in this study. Gougeon et al. performed a complex analysis on which equations best modeled the particle penetration in diffusion and interception ranges [27]. They found that Payet's model, Equation (1), best models the penetration in the diffusion regime, while Liu and Rubow's model, Equation (2), best models the penetration in the area where interception is dominant.

$$\eta_D = 1.6125\left(\frac{1-\alpha}{\mathrm{Ku}}\right)^{1/3} Pe^{-2/3} C_d C_d', \tag{1}$$

$$\eta_R = 0.615\,\frac{1-\alpha}{\mathrm{Ku}}\,\frac{N_R^2}{1+N_R}\,C_r, \tag{2}$$

where α is the filter fiber volume fraction (m^3/m^3), Ku is the Kuwabura hydrodynamic factor, Pe is the Peclet number, dimensionless, and N_R is the interception parameter, dimensionless. C_d and C_d' are the diffusion correction factors defined as

$$C_d = 1 + 0.388 Kn_f \left(\frac{(1-\alpha)Pe}{\mathrm{Ku}}\right)^{1/3},$$
$$C_d' = \frac{1}{1 + 1.6125(1-\alpha/\mathrm{Ku})^{1/3} Pe^{-2/3} C_d}, \tag{3}$$

where Kn_f is the Knudsen number (dimensionless) defined as

$$\mathrm{Kn}_f = \frac{2\lambda}{d_f}, \tag{4}$$

where λ is the gas molecule mean free path, 0.067 μm [26]. d_f is the fiber diameter (μm).

C_r is an interception correction factor defined as

$$C_r = 1 + \frac{1.996\mathrm{Kn}_f}{N_R}. \tag{5}$$

The remaining parameters are defined as the following:

$$Ku = a - \frac{a^2 + 2\ln(a) + 3}{4}. \tag{6}$$

a is the total filter media volume ($\mathrm{m}^3/\mathrm{m}^3$).

$$\mathrm{Pe} = \frac{1 \times 10^{-6} U d_f}{D_d}, \tag{7}$$

where U is the media face velocity (m/s). D_d is the particle diffusion coefficient (m^2/s).

$$N_R = \frac{D_p}{d_f}, \tag{8}$$

where D_p is the particle diameter (μm).

Once the diffusion and interception efficiencies are calculated, they must be used to calculate single-fiber deposition efficiency by the following equation:

$$\eta = 1 - (1 - \eta_D)(1 - \eta_R). \tag{9}$$

However, the $\eta_D \eta_R$ term is negligible compared to the $\eta_D + \eta_R$ term, and thus can be ignored. Hence, the single-fiber deposition efficiency now becomes

$$\eta = \eta_D + \eta_R. \tag{10}$$

Finally, the overall filter efficiency (E) based on particle size is defined as

$$E = L_u\left(1 - e^{-\eta S}\right), \tag{11}$$

where L_u is a multiplicative correction factor [8] and S is the fiber projected area, dimensionless, defined as

$$S = \frac{4L\alpha}{\pi d_f(1 - \alpha)} \tag{12}$$

where L is the length of filter media in direction of airflow (μm).

Additionally, Podgorski et al. had stated that pressure drop, Δp, can be estimated as

$$\frac{\Delta p}{L} = \frac{64\mu U}{d_f^2}\alpha^{3/2}\left(1 + 56\alpha^3\right). \tag{13}$$

The pressure drop created by the filter is due to its resistive force. The higher the pressure drop, the higher the force, and as a result, more energy is required to push the particles through the filter. As is well known, this force causes a change in the momentum of the particles. This is why a particle's speed is lower inside the media than the speed of the same particle before reaching the filter. In the treatment runs, there is an additional electrostatic force that is acting on the charged particles that also impacts the speed of particles in the filter media. This further reduces the particles' speed without causing any pressure drop. This allows for smaller size particles to be captured by the filter through diffusion and electrostatic force.

The equations above are for single-fiber filters; however, the majority of filters utilize multifibrous media, and thus there needs to be a way to model these kinds of filters. Kowalski et al. have developed such a method in which Equations (1) and (2) are calculated for each fiber [26]. Thus, any reference to fiber diameter, d_f, or fiber fractional volume, α, has now become specific to each individual fiber and must be calculated for every fiber in the filter. For instance, Equation (12) for the fiber project area would now become

$$S_i = \frac{4L\alpha_i}{\pi d_{f,i}(1 - \alpha_i)}. \tag{14}$$

Once the single-fiber efficiencies, η_i, and fiber projected area, S_i, are calculated for each of the fibers, the overall filter efficiency (Equation (11)),

$$E = 1 - e^{-\sum \eta_i S_i}. \tag{15}$$

It is now possible to vary the values for the fiber diameters and the fiber volume fractions for the filter efficiency curve to match the data from the experiments that were previously outlined. However, there are some restrictions used when varying these values. Most highly rated filters consist of fiber diameters between 0.65 and 6.5 μm, Kowalski et al. [26], so we restricted the fiber diameter values to be within this range. Additionally, the fiber volume fractions must all add to 1. For the purpose of this study, the assumption was made that there are three fibers with different fiber diameters. Table 1 summarizes the parameters used in modeling the efficiency curves.

However, fitting such a curve to the treatment data shows that there is not a strong correlation between the expected curve and the data. As shown in Figure 3, the treatment data with error bars does not look like a typical filter efficiency curve, and we can see that ionization effects diffusion and interception removal processes differently. So instead, for the purpose of getting agreement between theory and experiments, we chose to look at diffusion and interception efficiencies separately, varying the values for fiber

Table 1: Multifiber filter model parameters for diffusion and interception.

Parameters	Control diffusion	Control interception	Treatment 1 interception	Treatment 2 interception	Treatment 3 interception
Total volume fraction α	0.0020	0.0020	0.0020	0.0020	0.0020
Media length (m)	0.015	0.015	0.015	0.015	0.015
Nominal face velocity (FPM)	25	25	25	25	25
Media velocity (FPM)	3.118914308	3.118914308	3.118914308	3.118914308	3.118914308
Media velocity (m/s)	0.015840093	0.015840093	0.015840093	0.015840093	0.015840093
Fiber 1 diameter (microns)	3.32	2.00	0.771	0.80	0.827
Fiber 1 fraction of total α	0.33	0.94	0.44	0.60	0.57
Fiber 2 diameter (microns)	4.78	6.00	2.01	2.22	2.40
Fiber 2 fraction of total α	0.29	0.03	0.35	0.23	0.30
Fiber 3 diameter (microns)	6.45	6.50	5.75	5.60	6.50
Fiber 3 fraction of total α	0.38	0.03	0.21	0.17	0.13
Multiplication coefficient, L_u	1.00	0.95	0.965	0.93	0.946
r^2	0.89	0.82	0.98	0.98	0.96

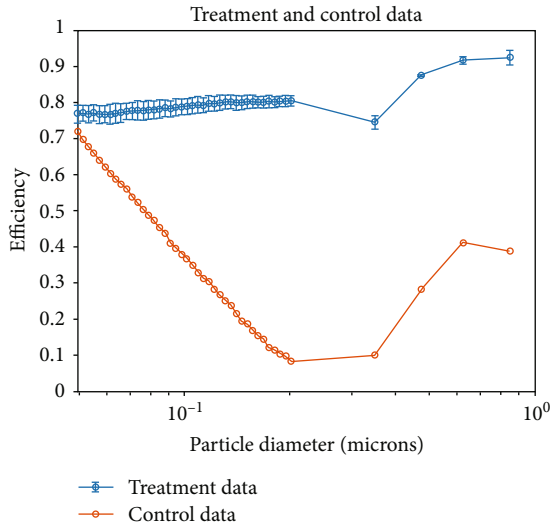

Figure 3: Removal efficiency of control versus treatment data.

diameters and fiber volume fractions to get as high of a correlation coefficient as possible between the curve and the data points. For the diffusion region, the correlation coefficient was determined from the data points between 49.6 nm and 350 nm, while for the interception efficiency, the value was determined from the data points between 350 nm and 850 nm. While the efficiency curve formula that was previously described could accurately model the diffusion region of the control data, the treatment data within the same region no longer behaved this way. Instead, it was found that a quadratic fit best modeled this portion of the treatment data. The parameters we found that best match our data are shown in Table 1. Once the diffusion and interception curves were optimized to best fit the data, the intersection between the curves was found, and a rolling average was taken from 10 nm from each side of the intersection point to smooth the curve.

With this new curve, we can accurately find the average efficiency by taking the area under the curve for a specific region and dividing that value by the difference between the highest and lowest particle diameter values in that region.

4. Results

These such curves are used to determine ratings for filters based on the removal efficiency for three different particle ranges: 0.3 to 1.0 μm, 1.0 to 3.0 μm, and 3.0 to 10.0 μm. For the purposes of the study, we are interested in finding the average efficiency between control and treatment data for these particle size ranges as well as the MPPS range. Once the optimized curves were developed, the curve was integrated to get the area underneath in order to find the average efficiency for a certain particle diameter range. This area was then divided by the difference between the highest and lowest particle diameters in that range. The process was done for each curve for the previously specified particle size ranges. The results of which are displayed in Table 2.

As can be seen from this table, there is a significant increase in filter removal efficiency in the 0.3-1 micron range, including the MPPS range, by implementing ionization. When considering the average efficiencies of the three treatment trials, there is a 275 percent increase in removal efficiency for the MPPS range of 100-500 nm.

5. Discussion

Substantial particle removal efficiency was achieved by implementing an ionizer to produce 20,000 ± 500 positive and negative ions prior to the cigarette smoke being introduced into the chamber. Once the smoke was introduced, the ion count drastically decreased since the ions were polarizing the smoke particles which led to the agglomeration of these particles. There was a 134 percent increase in the removal efficiency of particles in the 0.3-1.0 micron range

Table 2: Combined diffusion and interception average efficiency data.

	Control	Treatment 1	Treatment 2	Treatment 3	Average treatment
Overall r^2	0.87	0.99	0.97	0.98	N/A
0.3-1 micron	0.384	0.899	0.888	0.887	0.892
1-3 micron	0.847	0.965	0.930	0.946	0.947
3-10 micron	0.949	0.965	0.930	0.946	0.947
MPPS value (microns)	0.2956	0.3417	0.3421	0.3403	0.3414
MPPS efficiency	0.221	0.797	0.818	0.790	0.802

when ionization was used and a 275 percent increase in the MPPS range of 100-500 nm (Table 2). It was observed that with the use of ionization, the most penetrating particle size had increased in diameter. Thus proving that when the particles present in the air are ionized with both positive and negative charges, the attraction-repulsion dynamic results in the coagulation of particles with opposite charges, leading to a higher concentration of larger diameter particles. These larger particles are then more easily captured by the filter either through interception or electrostatic attraction. However, even the most efficient filters have a most penetrating particle size, which ionization can help improve the capture efficiency.

Additionally, larger particles are subjected more to gravitational force since they have a higher mass. Thus, if the gravitational force exerted on the particle is greater than the electric force, then the particle is more likely to deposit onto a surface rather than the filter.

As previously stated, every filter creates a pressure drop caused by its resistive force. Typically, more efficient filters are more fibrous and thus have a higher resistive force which creates a greater pressure drop. This force decreases a particle's momentum within the filter which results in a lower velocity of the particle through the filter. This lower velocity allows for smaller particles to be more easily captured through the diffusion process. Through the use of bipolar ionization, there is an additional electrostatic force that is acting on the charged particles. This force opposes the motion of the particles and thus further reduces the speed of the particles within the filter media. Smaller size particles are more easily captured through diffusion and electrostatic force. Therefore, as shown, the use of a bipolar ionizer improves a filter's removal efficiency to that of a higher-rated filter without increasing the resistive force. The resultant pressure drop across the filter remains the same, and the energy required to push particles through the filter is the same.

6. Conclusion

The results of this study confirm that bipolar ionization increases a mechanical filter's removal efficiency of fine and ultrafine particles from indoor environments as well and more information on how ionization affects the most penetrating particle sizes. The ionizer used in this study produced an average 275% increase in the removal efficiency of the MPPS range after 18 minutes when compared to the control. Therefore, the use of bipolar ions to help clean indoor air has proven to be an effective method. This process can then be applied and tested in cleaning efficiencies for other air pollutants such as wildfire smoke. In areas where there are many and spontaneous wildfires, this technology can be especially useful.

Data Availability

Unfortunately, due to a nondisclosure agreement (third-party agreement) between the authors and collaborators, the authors cannot disclose the data.

Conflicts of Interest

The authors declare that they have no conflicts of interest.

Acknowledgments

The authors would like to acknowledge the financial support of GPS Air in conducting this research. Pranav Muthukrishnan would like to thank GPS Air for a Summer Internship.

References

[1] S. S. Lim, T. Vos, A. D. Flaxman, G. Danaei, K. Shibuya, and H. Adair-Rohani, "A comparative risk assessment of burden of disease and injury attributed to 67 risk factors and risk factor clusters in 21 regions, 1990-2010: A systematic analysis for the global burden of disease study 2010," *The Lancet*, vol. 380, no. 9859, pp. 2224–2260, 2013.

[2] World Health Organization, *World Report on Knowledge for Better Health: Strengthening Health Systems*, World Health Organization, 2004.

[3] D. E. Horton, C. B. Skinner, D. Singh, and N. S. Diffenbaugh, "Occurrence and persistence of future atmospheric stagnation events," *Climatic Change*, vol. 4, no. 8, pp. 698–703, 2014.

[4] G. Sérafin, P. Blondeau, and C. Mandin, "Indoor air pollutant health prioritization in office buildings," *Indoor Air*, vol. 31, no. 3, pp. 646–659, 2021.

[5] S. N. Rudnick, "Optimizing the design of room air filters for the removal of submicrometer particles," *Aerosol Science and Technology*, vol. 38, no. 9, pp. 861–869, 2004.

[6] "Why wildfire smoke is a health concern," https://www.epa.gov/wildfire-smoke-course/why-wildfire-smoke-health-concern.

[7] E. Alonso-Blanco, A. I. Calvio, R. Fraile, and A. Castro, "The influence of wildfires on aerosol size distributions in rural

areas," *The Scientific World Journal*, vol. 2012, Article ID 735697, 13 pages, 2012.

[8] W. J. Kowalski and W. Bahnfleth, "Merv filter models," 2002, https://www.nafahq.org/merv-filter-models/.

[9] A. Podgórski, A. Bałazy, and L. Gradoń, "Application of nanofibers to improve the filtration efficiency of the most penetrating aerosol particles in fibrous filters," *Chemical Engineering Science*, vol. 61, no. 20, pp. 6804–6815, 2006.

[10] Z. Grabarczyk, "Effectiveness of indoor air cleaning with corona ionizers," *Journal of Electrostatics*, vol. 51-52, pp. 278–283, 2001.

[11] J. Černecký, K. Valentová, E. Pivarčiová, and P. Božek, "Ionization impact on the air cleaning efficiency in the interior," *Measurement Science Review*, vol. 15, no. 4, pp. 156–166, 2015.

[12] B. Pushpawela, R. Jayaratne, A. Nguy, and L. Morawska, "Efficiency of ionizers in removing airborne particles in indoor environments," *Journal of Electrostatics*, vol. 90, pp. 79–84, 2017.

[13] S. A. Grinshpun, A. Adhikari, B. U. Lee, M. Trunov, and E. A. G. Mainelis, "Indoor air pollution control through ionization," *WIT Transactions on Ecology and the Environment*, vol. 74, 2004.

[14] J.-H. Park, K.-Y. Yoon, Y.-S. Kim, J. H. Byeon, and J. Hwang, "Removal of submicron aerosol particles and bioaerosols using carbon fiber ionizer assisted fibrous medium filter media," *Journal of Mechanical Science and Technology*, vol. 23, no. 7, pp. 1846–1851, 2009.

[15] J. H. Park, K. Y. Yoon, and J. Hwang, "Removal of submicron particles using a carbon fiber ionizer-assisted medium air filter in a heating, ventilation, and air-conditioning (HVAC) system," *Building and Environment*, vol. 46, no. 8, pp. 1699–1708, 2011.

[16] M. Smith, K. Lee, and T. Matsoukas, "Coagulation of charged aerosols," *Journal of Nanoparticle Research*, vol. 1, no. 2, pp. 185–195, 1999.

[17] S. M. Charan, W. Kong, R. C. Flagan, and J. H. Seinfeld, "Effect of particle charge on aerosol dynamics in Teflon environmental chambers," *Aerosol Science and Technology*, vol. 52, no. 8, pp. 854–871, 2018.

[18] F. Farahi, "Soft ionization: improving indoor air quality," *IEEE Transactions on Industry Applications*, pp. 1–7, 2023.

[19] EPA, "Particle pollution exposure," https://www.epa.gov/pmcourse/particle-pollution-exposure.

[20] "Center for tobacco reference products," https://ktrdc.ca.uky.edu/Reference-Products.

[21] "Aeolus corporation," https://aeoluscorp.com/.

[22] N. E. Klepeisn, M. Apte, L. A. Gundel, R. G. Sextro, and W. W. Nazaroff, "Determining size-specific emission factors for environmental tobacco smoke particles," *Aerosol Science and Technology*, vol. 37, no. 10, pp. 780–790, 2003.

[23] D. Mueller, J. Schulze, H. Ackermann, D. Klingelhoefer, S. Uibel, and D. A. Groneberg, "Particulate matter (pm) 2.5 levels in ets emissions of a Marlboro red cigarette in comparison to the 3r4f reference cigarette under open- and closed-door condition," *Journal of Occupational Medicine and Toxicology*, vol. 7, no. 1, p. 14, 2012.

[24] X. Tang, Z. Zheng, H. S. Jung, and A. Asa-Awuku, "The effects of mainstream and sidestream environmental tobacco smoke composition for enhanced condensational droplet growth by water vapor," *Aerosol Science and Technology*, vol. 46, no. 7, pp. 760–766, 2012.

[25] M. Forster, J. McAughey, K. Prasad, E. Mavropoulou, and C. Proctor, "Assessment of tobacco heating product thp1.0. Part 4: characterisation of indoor air quality and odour," *Regulatory Toxicology and Pharmacology*, vol. 93, pp. 34–51, 2018.

[26] W. J. Kowalski, W. P. Bahnfleth, and T. S. Whittam, "Filtration of airborne microorganisms: modeling and prediction," *ASHRAE Transactions*, vol. 105, 1999.

[27] R. Gougeon, D. Bouland, and A. Renoux, "Comparison of data from model fiber filters with diffusion, interception and inertial deposition models," *Chemical Engineering Communications*, vol. 151, no. 1, pp. 19–39, 1996.